

## Active control of flow-induced vibration from bluff-body wakes: the response of an elastically-mounted cylinder to rotational forcing

J. S. Leontini<sup>1</sup>, and M. C. Thompson<sup>1</sup>

<sup>1</sup>Fluids Laboratory for Aeronautical and Industrial Research (FLAIR)  
Department of Mechanical and Aerospace Engineering  
Monash University, Victoria 3800, Australia

### Abstract

This paper investigates the flow past an elastically-mounted cylinder, constrained to oscillate in the cross-stream direction, which is then externally forced to perform rotational oscillations. The motivation for this study is the enhancement of cross-stream oscillations of the body. These oscillations can be used to drive a generator, and therefore used as a renewable energy technology. More generally, this forcing is treated as an open-loop control strategy of the wake and the resulting cylinder oscillations.

The system tested is such that its natural structural frequency,  $f_n$ , is close to the vortex shedding frequency from a stationary cylinder. This means that with no forcing, the cylinder oscillations, and the periodic vortex shedding that characterizes the wake, are synchronized.

Numerical simulations have been conducted for a range of forcing frequencies  $f_n/2 \leq f_d \leq 2f_n$ , and the effect of the forcing on this base, synchronized case determined. It is shown that the forcing can significantly increase the peak oscillation amplitude, and that the wake and cylinder cross-stream oscillation remains synchronized to the rotational driving over a significant range of driving frequencies. Outside of this synchronized range, the flow is shown to be typically quasiperiodic, with modulated oscillations around the system natural structural frequency.

### Introduction

Slender bodies with bluff cross sections, such as cylinders, immersed in a freestream with their axis perpendicular to the flow, susceptible to a range of flow-induced vibration (FIV) phenomena. For circular cylinders, which do not have a defined angle of attack, the most likely phenomenon to occur is vortex-induced vibration (VIV). This occurs due to periodic vortex shedding in the wake. This periodic shedding (where a vortex is shed from one side of the body, then a vortex of opposite sign is shed from the other side of the body, forming the ubiquitous Kármán vortex street) generates a periodic loading on the cylinder in the cross-stream direction. When this vortex shedding frequency is close to a natural structural frequency, large-amplitude oscillations can occur in a resonance-type response. Moreover, the vortex shedding frequency will change to match or synchronize with the body oscillation frequency, leading to large, periodic oscillations.

A focus of recent research has been harnessing these oscillations as a potential renewable energy source [2, 1]. For this to be viable, control methods that maximize the energy transfer from the flow to the structure need to be investigated.

The control strategies available are numerous, but can be broken into two main categories. Closed-loop control relies on taking a measurement of the flow that in some way represents its global behaviour (practically, this means measuring at a point

or set of points with a probe or pressure tap) and varying some kind of control forcing (such as driving the body) based upon these measurements. Open-loop control does not have this feedback loop, and instead the control forcing is prescribed. While closed-loop control offers greater flexibility, open-loop control is far simpler, and often more practical in engineering applications.

Open-loop control can be further divided into passive and active methods. Passive methods require no energy input, and are typically based on geometric changes, such as adding strakes, bumps, or varying the angle of attack.

With regard to cylinder wakes (which are nominally two-dimensional, or at least dominated by two-dimensional structures), a number of studies exist investigating active open-loop control methods, especially those based on harmonically forcing the body in one particular degree of freedom. These include forcing in the cross-stream direction [3, 9, 18, 4, 11], the streamwise direction [7, 12, 5, 10], and rotational forcing [8, 13, 15, 16, 6]. Two common themes arise from these studies. First, the wake can be synchronized to the forcing, resulting in a purely periodic flow with high spanwise correlation, over particular bands of forcing frequencies. Second, these bands of frequencies are essentially governed by the spatio-temporal symmetry of the forcing as compared to the spatio-temporal frequency of the unforced Kármán vortex street. The consequence of these two results is that forcing of the body that respects the symmetry  $u(x, y, t) = u(x, -y, t + T/2)$ , where  $u$  is a velocity component,  $x$  and  $y$  spatial coordinates,  $t$  is time and  $T$  is the period of the forcing, will typically see synchronization of the flow to the forcing when the frequency of the forcing is close to the vortex shedding frequency (or Strouhal frequency  $f_{St}$ ) of the unforced system.

In this paper, the concept of wake control by harmonic forcing is extended to the control of VIV. The forcing using is oscillatory rotation of the cylinder. The complicating factor in VIV is the interaction between the wake and the body that naturally occurs. Rather than an interaction between the driving frequency  $f_d$  and the Strouhal frequency  $f_{St}$ , there is three-way interaction between  $f_d$ ,  $f_{St}$ , and the natural structural frequency  $f_n$ . For this reason,  $f_n$  is set to a value close to  $f_{St}$  so that the unforced system has the vortex shedding and body motion synchronized. The amplitude of the forcing is fixed to a value large enough to ensure a significant impact on the flow. The forcing frequency is then systematically varied and the response of the system quantified. Very large periodic oscillations of the body are recorded that are shown to be amenable to energy generation.

### Methodology

Two-dimensional simulations have been conducted using a spectral element code solving the incompressible Navier-Stokes equations. The accelerating frame of reference is attached to the cylinder, the acceleration found by solving the simple harmonic equation of motion of the elastically-mounted cylinder. The use

of this method means no mesh deformation is required to account for the body motion. Details of the method and its use for similar problems can be found in [17, 11]. The prescribed oscillatory rotation is implemented simply by prescribing the tangential velocity on the surface of the cylinder over time.

The rotational forcing is prescribed by the function

$$\theta = A^* \sin(2\pi f_d \tau), \quad (1)$$

where  $\theta$  is the angular displacement of the cylinder surface,  $A^*$  is the amplitude of the oscillation in radians, and  $f_d$  is the nondimensional forcing or driving frequency  $f_d = fD/U$ , where  $f$  is the forcing frequency. All simulations used an amplitude  $A^* = \pi/2$ , resulting in peak-to-peak oscillations of a half a rotation. The Reynolds number  $Re = UD/\nu$ , where  $U$  is the freestream velocity,  $D$  is the cylinder diameter, and  $\nu$  is the kinematic viscosity, is fixed at  $Re = 200$ . The natural frequency *in vacuo*,  $f_n = \sqrt{k/m}/(2\pi)$ , where  $k$  is the spring stiffness coefficient, and  $m$  is the mass of the body, is fixed at  $f_n = 0.2$ . The mass ratio  $m^* = m/m_f$ , where  $m_f$  is the mass of the fluid displaced by the body, is set to  $m^* = 1$ . No mechanical damping has been added to the system.

## Results

Figure 1 shows the maximum amplitude of oscillation as a function of the driving frequency  $f_d$ . The driving frequency spans the range  $f_n/2 \leq f_d \leq 2f_n$ . It is clear that the forcing has a huge influence on the amplitude, with oscillations up to 300% larger occurring with respect to the unforced case. This maximum amplitude occurs at  $f_d \simeq 0.14$ , or for a forcing frequency around 70% of  $f_n$ .

An intriguing feature of the system shown in figure 1 is the response when  $f_d = f_n$ . It might be expected that when these two frequencies coincide, the amplitude would be largest through a resonance-type response. However, figure 1 shows that the amplitude is essentially unaffected by the forcing at this frequency, with a minor decrease with respect to the unforced case.

The observation of very large amplitudes for low frequency forcing, and unaffected amplitude for forcing at  $f_n$ , seem to be explained by considering the spacing of the shed vortices in the wake. A classic inviscid result from von Kármán discussed further by [14] is that the ratio of the lateral to longitudinal spacing of vortices in the Kármán wake tends towards a preferred value of around 0.281. If the vortex shedding is reduced in frequency, but the convection speed of a given vortex remains the same, the longitudinal spacing between vortices will increase. To maintain the spacing ratio, this increase in longitudinal spacing must result in an increase in lateral spacing. The further a vortex is moved laterally, the more transverse force it will exert on the cylinder. A larger transverse force could reasonably be expected to result in larger amplitude oscillation, as is observed at low frequencies. The same argument says that if the frequency is unchanged (as occurs when  $f_d = f_n$ ), the vortex spacing in unchanged, and the transverse force and therefore amplitude of oscillation is unchanged.

This argument only applies for as long as the wake and vortex shedding is synchronized with the oscillatory driving. Figure 2 shows the frequency content of the measured lift force as a function  $f_d$ . The plot was created by taking the frequency spectrum of the lift force history for each value of  $f_d$  and stacking them next to each other. For each value of  $f_d$ , the power in the spectrum has been normalized by the maximum power. This means that the power for a given frequency component cannot be directly compared across  $f_d$ , but it gives a very clear picture of which frequencies are dominant in the response as a function of  $f_d$ .

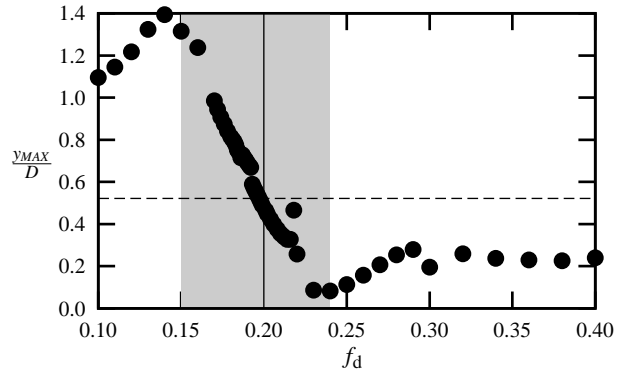


Figure 1: The peak amplitude of transverse oscillation as a function of the driving frequency  $f_d$ . The solid vertical line marks  $f_n$ , the dotted horizontal line marks the amplitude of the unforced case. The gray shaded region marks the range of  $f_d$  for which the wake is synchronized with the driving.

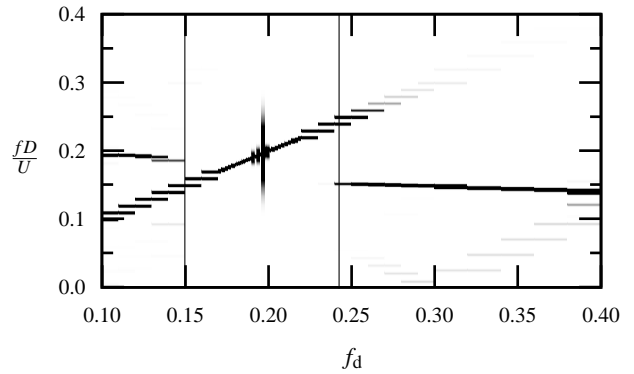


Figure 2: Frequency content of the lift force as a function of the driving frequency. The frequency content for a given value of  $f_d$  was determined using a Fourier transform, and then the spectra for all values of  $f_d$  stacked next to each other. The spectrum for each value of  $f_d$  has been normalized by the maximum power in the spectrum. The plot shows that the flow is dominated by the driving frequency over the range  $0.14 < f_d < 0.24$ , and governed by the driving frequency and a second frequency related to the natural frequency outside of this range.

It is clear that over the range  $0.14 < f_d < 0.24$ , the frequency response of the wake is dominated by the driving frequency. Either side of this range the frequency response primarily consists of the driving frequency, and a second frequency that is close to, but lower than, the driving frequency. This second frequency decreases as the frequency of the driving increases. This appears to be an added mass effect, where the entrained fluid in a layer near the body acts as mass that needs to be moved by the oscillating body. This means the apparent mass of the body is larger than its actual mass, and therefore the natural frequency is lowered.

Images of instantaneous snapshots of the wake are shown in figure 3. A series of images are shown over a range of driving frequencies where the wake is synchronized to the driving. This series shows that with increasing driving frequency, the lateral and longitudinal spacing of the wake vortices decreases, resulting in smaller transverse forces, in agreement with the argument outlined above.

With respect to energy generation, large oscillations are only of use if they are in phase with the force producing them. Only in this way do the forces impart work on the structure, and hence

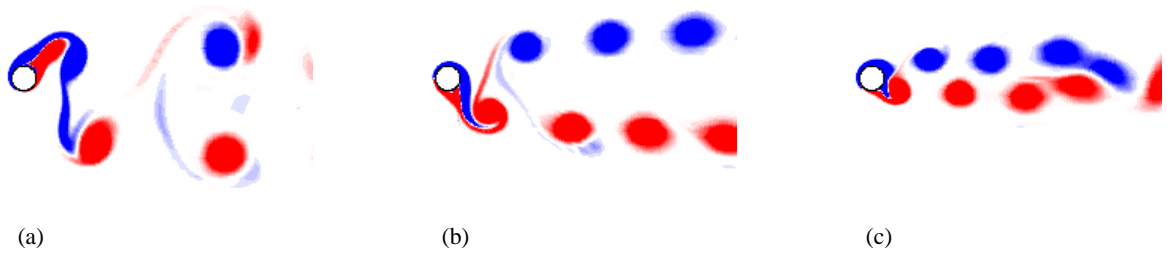


Figure 3: Snapshots of the wake over a range of driving frequencies: (a)  $f_d = 0.15$ ; (b)  $f_d = 0.20$ , (c)  $f_d = 0.24$ . Colour contours are of vorticity between levels  $\pm 1$ . The images show that with increasing frequency, the lateral and longitudinal spacing of the wake vortices decreases, resulting in smaller transverse forces.

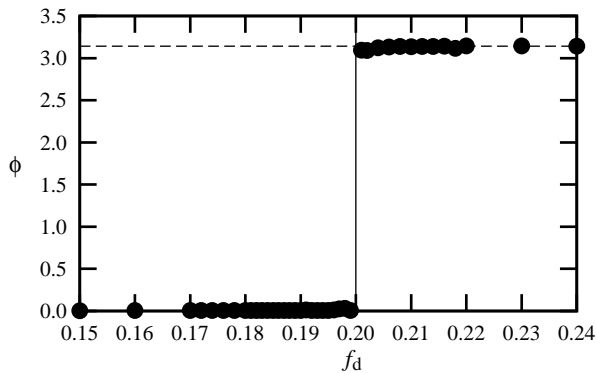


Figure 4: The average phase between the lift force and the transverse body oscillation, over the range of driving frequencies for which the flow remains synchronized to the driving. The solid vertical line marks  $f_n$ , the dotted horizontal line marks a phase of  $\phi = \pi$ . The phase remains close to zero where the amplitudes of oscillation are the biggest, favourable for energy transfer.

transfer energy from the flow to the structure. Therefore, a measured phase between the lift (transverse) force and the body transverse oscillation  $\phi \simeq 0$  is favourable for energy transfer, while a phase  $\phi \simeq \pi$  indicates close to no work can be done on the cylinder.

Figure 4 plots this phase  $\phi$  over the range of driving frequencies where the flow is synchronized to the driving frequency. The phase  $\phi$  was calculated by finding the maximum of the cross-correlation between the two signals. It shows that for driving frequencies less than the natural frequency,  $f_d < f_n$ , the phase remains very close to zero. However, for  $f_d \geq f_n$ , there is a phase jump to  $\phi \simeq \pi$ .

This result, coupled with the results shown in figure 1 that the amplitude of oscillation is greatest for the lowest frequencies in the synchronized range, indicates that significant increases in energy transfer from the fluid to the structure, with respect to the unforced case, are possible using oscillatory oscillation. Of course, this oscillation comes at an energy cost, and it remains to be seen if the increase in energy transfer from the fluid to the body offsets the cost of the control (this cannot be directly measured from the current simulations as the actual energy transfer is, and must, be zero, as there is no mechanical damping to dissipate energy). However, it can be shown that as the driving frequency decreases, the energy required for the control also decreases.

Figure 5 shows the work done by the rotation of the cylinder

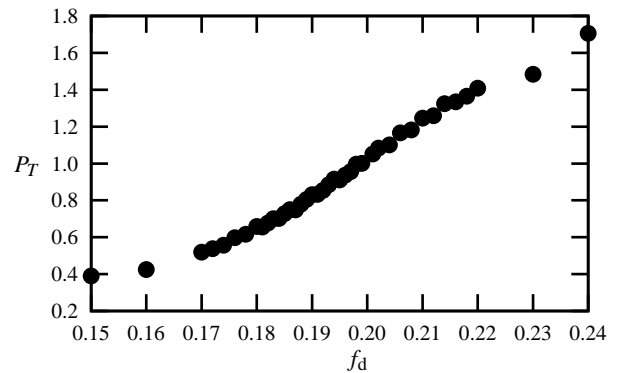


Figure 5: The average power required for the rotational control over a period of oscillation, as a function of the driving frequency. This shows that low frequencies of driving, where the amplitudes of transverse oscillation are greatest (and potential energy generation is the highest), cost the least in terms of energy.

on the fluid per period of oscillation. This is calculated by taking the negative of the integral of the product of the torque and the cylinder angular velocity over one period of oscillation, and normalizing by the period of oscillation, according to the formula

$$P_T = \frac{1}{T} \int_{\tau}^{\tau+T} M \cdot \omega d\tau, \quad (2)$$

where  $P_T$  is the nondimensional average power,  $T$  is the period of the forcing,  $\tau$  is nondimensional time,  $M$  is the moment or torque, and  $\omega$  is the angular velocity of the cylinder. The figure shows that the power required for the control increases approximately quadratically with the driving frequency, but most importantly is smallest where the recorded amplitudes of oscillation are the largest.

## Conclusions

The results of this paper show that the rotational oscillation of an elastically-mounted cylinder can have significant consequences for the flow and resulting transverse oscillations. Very large oscillations, with a phase such that energy transfer from the flow to the structure is highly likely, can be obtained for a relatively small energy cost. It is therefore concluded that rotational oscillation is a promising open-loop control strategy for the optimization of energy generation devices based on vortex-induced vibration.

## Acknowledgements

This work was financially supported by the Australian Research Council (ARC) through project DP110102141 as part of the Discovery Projects scheme. JL acknowledges the financial support of the ARC through an Australian Postdoctoral Fellowship (APD).

## References

- [1] Barrero-Gil, A., Pindado, S. and Avila, S., Extracting energy from vortex-induced vibrations: a parametric study, *App. Math. Modelling*, **36**, 2012, 3153–3160.
- [2] Bernitsas, M. M., Ben-Simon, Y., Raghavan, K. and Garcia, E. M. H., The VIVACE converter: model tests at high damping and Reynolds number around  $10^5$ , *J. Offshore Mech. & Arctic Eng.*, **131**, 2009, 011102–1.
- [3] Bishop, R. E. D. and Hassan, A. Y., The lift and drag forces on a circular cylinder oscillating in a flowing fluid, *Proceedings of the Royal Society of London, series A*, **277**, n1368, 1964, 51–75.
- [4] Blackburn, H. M. and Henderson, R., A study of two-dimensional flow past an oscillating cylinder, *J. Fluid Mech.*, **385**, 1999, 255–286.
- [5] Cetiner, O. and Rockwell, D., Streamwise oscillations of a cylinder in a steady current. Part 1. Locked-on states of vortex formation and loading, *J. Fluid Mech.*, **427**, 2001, 1–28.
- [6] D’Adamo, J., Godoy-Diana, R. and Wesfried, J. E., Spatiotemporal spectral analysis of a forced cylinder wake, *Phys. Rev. E*, **84**, 2011, 056308.
- [7] Griffin, O. M. and Ramberg, S. E., Vortex shedding from a cylinder vibrating in line with an incident uniform flow, *J. Fluid Mech.*, **75**, 1976, 257–271.
- [8] He, J.-W., Glowinski, R., Metcalfe, R., Nordlander, A. and Periaux, J., Active control and drag optimization for flow past a circular cylinder, *J. Comp. Phys.*, **163**, 2000, 83–117.
- [9] Koopman, G. H., The vortex wakes of vibrating cylinders at low Reynolds numbers, *J. Fluid Mech.*, **28**, 1967, 501–512.
- [10] Leontini, J. S., Lo Jacono, D. and Thompson, M. C., A numerical study of an inline oscillating cylinder in a free stream, *J. Fluid Mech.*, **688**, 2011, 551–568.
- [11] Leontini, J. S., Stewart, B. E., Thompson, M. C. and Hourigan, K., Wake-state and energy transitions of an oscillating cylinder at low Reynolds number, *Phys. Fluids*, **18**, no. 6, 2006, 067101.
- [12] Ongoren, A. and Rockwell, D., Flow structure from an oscillating cylinder Part 2. Mode competition in the near wake, *J. Fluid Mech.*, **191**, 1988, 225.
- [13] Poncet, P., Topological aspects of three-dimensional wakes behind rotary oscillating cylinders, *J. Fluid Mech.*, **517**, 2004, 27–53.
- [14] Saffman, P. G. and Schatzman, J. C., An inviscid model for the vortex-street wake, *J. Fluid Mech.*, **122**, 1982, 467–486.
- [15] Thiria, B., Goujon-Durand, S. and Wesfried, J. E., The wake of a cylinder performing rotary oscillations, *J. Fluid Mech.*, **560**, 2006, 123–147.
- [16] Thiria, B. and Wesfried, J. E., Physics of temporal forcing in wakes, *J. Fluids & Structures*, **25**, 2009, 654–665.
- [17] Thompson, M. C., Hourigan, K. and Sheridan, J., Three-dimensional instabilities in the wake of a circular cylinder, *Exp. Therm. Fluid Sci.*, **12**, 1996, 190–196.
- [18] Williamson, C. H. K. and Roshko, A., Vortex formation in the wake of an oscillating cylinder, *J. Fluids & Structures*, **2**, 1988, 355–381.